AIP | Physics of Plasmas
#1 JOURNAL IN 2014 GOOGLE SCHOLAR METRICS FOR THE PLASMA & FUSION CATEGORY

Nonlinear coupling between breathing and quadrupole-like oscillations in the transport of mismatched beams in continuous magnetic focusing fields

W. Simeoni Jr., F. B. Rizzato, and R. Pakter

Citation: Physics of Plasmas **13**, 063104 (2006); doi: 10.1063/1.2208293
View online: http://dx.doi.org/10.1063/1.2208293
View Table of Contents: http://scitation.aip.org/content/aip/journal/pop/13/6?ver=pdfcov
Published by the AIP Publishing

Articles you may be interested in

Effect of image charge on the off-axis transport of intense beams in a small aperture quadrupole lattice
Phys. Plasmas **20**, 103119 (2013); 10.1063/1.4826509

Studies of space-charge-dominated multispecies beam in a solenoid based beam transport line
Phys. Plasmas **19**, 113112 (2012); 10.1063/1.4768457

Fast ignition by laser driven particle beams of very high intensity
Phys. Plasmas **14**, 072701 (2007); 10.1063/1.2748389

Particle manipulation with nonadiabatic ponderomotive forcesa)
Phys. Plasmas **14**, 055901 (2007); 10.1063/1.2436149

Formation of nonlinear magnetic islands via trapped electrons in the lower-hybrid range
Phys. Plasmas **11**, 4946 (2004); 10.1063/1.1795197

Reuse of AIP Publishing content is subject to the terms at: https://publishing.aip.org/authors/rights-and-permissions. Downloaded to IP: 143.54.44.137 On: Wed, 04 May 2016 17:19:57

Nonlinear coupling between breathing and quadrupole-like oscillations in the transport of mismatched beams in continuous magnetic focusing fields

W. Simeoni, Jr.,[a] F. B. Rizzato,[b] and R. Pakter[c]
Instituto de Física, Universidade Federal do Rio Grande do Sul, Caixa Postal 15051, 91501-970, Porto Alegre, RS, Brazil

(Received 19 December 2005; accepted 5 May 2006; published online 14 June 2006)

A nonlinear analysis of the transport of breathing beams considering nonaxisymmetric perturbations is performed. It is shown that large-amplitude breathing oscillations of an initially round beam may couple nonlinearly to quadrupole-like oscillations, such that the excess energy initially constrained to the axisymmetric breathing oscillations is allowed to flow back and forth between breathing and quadrupole-like oscillations. In this case, the beam develops an elliptical shape with a possible increase in its size along one direction as the beam is transported. This is a highly nonlinear phenomenon that occurs for large mismatch amplitudes on the order of 100% and is found to be particularly relevant for space-charge-dominated beams with $K \gtrsim k_0 \epsilon$, where K is the beam perveance, k_0 is the vacuum phase advance per unit axial length, and ϵ is the emittance of the beam. A simple model based on mapping techniques is used to clarify the mechanism that leads to the energy exchange between the modes and is tested against results from direct integration of the envelope equations. © *2006 American Institute of Physics*. [DOI: 10.1063/1.2208293]

I. INTRODUCTION

There has been a lot of interest in the research of high-intensity accelerators and vacuum electronic devices in order to meet the needs in areas such as communication, heavy-ion fusion, and basic science research. A key issue to be overcome in the development of these devices is the prevention of particle beam losses[1,2] because they lower energy efficiency and may be responsible for activation of the walls surrounding the beam in accelerators[3] and pulse shortening[4] due to secondary electron emission in high-power microwave sources. In order to achieve that, a crucial ingredient is a better understanding of the beam transport stability. In that regard, many studies have been made since the 1980s on the linear stability of uniform and periodically focused beams, where vanishing small deviations from the matched (equilibrium) solution were taken into account.[5–11] They detected the occurrence of different instability modes which compromise beam transport for certain parameters of the system. Of particular relevance for axisymmetric solenoidal focusing is the breathing mode that induces increasing-amplitude axisymmetric oscillations of the beam envelope around its matched (equilibrium) value; and the quadrupole-like mode that induces elliptic oscillations of the beam, breaking its symmetry.[6,9,10] Studies of beams with finite mismatch amplitude based both on collective mode analysis[12–14] and on test-particle dynamics[15,16] were also performed, but the results are restricted to axisymmetric beams. In particular, it was shown that finite amplitude breathing modes may induce instabilities, chaotic envelope dynamics, and halo formation.

In this paper, we perform a nonlinear analysis of the transport of beams in continuous magnetic focusing fields taking into consideration nonaxisymmetric effects. In particular, we investigate the nonlinear coupling between breathing modes and quadrupole-like modes based on envelope equations. It is shown that large-amplitude breathing oscillations caused by some sort of mismatch may nonlinearly couple to quadrupole-like oscillations for an initially *quasi*-axisymmetric beam. In this case, the excess energy initially constrained to the axisymmetric breathing oscillations is allowed to flow back and forth between breathing and quadrupole-like oscillations, with the beam developing an elliptical shape with a possible increase in its size along one direction as the beam is transported. Generally, this may induce beam losses, which are enhanced if conducting wall effects are taken into account,[17] and may also induce a detuning in the wave-beam interaction in high-power microwave tubes. This nonlinear process is found to be particularly relevant for space-charge-dominated beams with $K \gtrsim k_0 \epsilon$, where K is the beam perveance, k_0 is the vacuum phase advance per unit axial length, and ϵ is the emittance of the beam, and occurs for large mismatch amplitudes on the order of 100%, which are compatible, for instance, to mismatches induced by current oscillations in high-power microwave sources.[18] A simple model is developed to clarify the basic mechanism that leads to the energy exchange between the modes and is numerically tested against results obtained from direct integration of the envelope equations.

The paper is organized as follows. In Sec. II, the model equations are introduced and a simple model based on mapping techniques is developed to clarify the basic mechanism that leads to energy exchange between breathing and quadupole-like modes for large-amplitude mismatched beams. In Sec. III, results obtained by direct integration of

[a]Electronic mail: wsjr@if.ufrgs.br
[b]Electronic mail: rizzato@if.ufrgs.br
[c]Electronic mail: pakter@if.ufrgs.br

 © 2006 American Institute of Physics

Reuse of AIP Publishing content is subject to the terms at: https://publishing.aip.org/authors/rights-and-permissions. Downloaded to IP: 143.54.44.137 On: Wed, 04 May 2016 17:19:57

the envelope equations are presented and compared to results from the simple model. In Sec. IV, the paper is concluded.

II. THE MODEL EQUATIONS

A. Envelope equations and the matched solution

We consider an axially long unbunched beam propagating with constant average axial velocity $\beta_b c\hat{\mathbf{e}}_z$ along a uniform solenoidal magnetic focusing field $\mathbf{B}(\mathbf{x})=B_z\hat{\mathbf{e}}_z$, where c is the speed of light *in vacuo* and B_z is constant. Since we are dealing with solenoidal focusing, it is convenient to work in the Larmor frame of reference,[8] which rotates with respect to the laboratory frame with angular velocity $\Omega_L=qB_z/2\gamma_b mc$, where q, m, and $\gamma_b=(1-\beta_b^2)^{-1/2}$ are, respectively, the charge, mass, and relativistic factor of the beam particles. The beam is assumed to have an elliptical cross section centered at $x=0=y$ and vanishing canonical angular momentum $P_\theta\equiv\langle xy'-yx'\rangle=0$, where x and y are the positions of the beam particles in the Larmor frame, the prime denotes derivative with respect to s, and $\langle\cdots\rangle$ represents average over beam particles. Although we restrict our analysis to a uniform focusing, the results are expected to be valid for periodic focusing as well, as long as $P_\theta=0$ and smooth-beam approximations are valid.[8] In the paraxial approximation, the equations that dictate the beam envelope evolution are

$$\frac{d^2a}{ds^2}+k_0^2a-\frac{2K}{a+b}-\frac{\epsilon^2}{a^3}=0, \tag{1}$$

$$\frac{d^2b}{ds^2}+k_0^2b-\frac{2K}{a+b}-\frac{\epsilon^2}{b^3}=0, \tag{2}$$

where $s=z$ is the propagation distance, a and b are the ellipsis semi-axes radii, $k_0=qB_z/2\gamma_b\beta_b mc^2$ is the vacuum phase advance per unit axial length that measures the focusing field strength, $K=2q^2N_b/\gamma_b^3\beta_b^2mc^2$ is the beam perveance, N_b is the number of particles per unit axial length, and ϵ is the unnormalized emittance of the beam. Equations (1) and (2) can be derived in different frameworks, for instance from a kinetic Vlasov-Maxwell description or by taking successive momenta of a single particle equation of motion along with convenient closure relations.[8] In the former case, $a(s)$ and $b(s)$ are the exact outermost radii of an uniform distribution Kapchinskij-Vladimirskij equilibrium beam,[19] whereas in the latter, they are related to rms beam sizes along the x and y axes.[20]

It is easy to verify that there is a particular solution of the envelope equations (1) and (2) for which $a(s)=b(s)=r_{b0}=\text{const}$. This corresponds to the so-called matched solution for which a circular beam of radius r_{b0} preserves its shape throughout the transport along the focusing field. The matched radius is

$$r_{b0}=\left[\frac{K+(K^2+4k_0^2\epsilon^2)^{1/2}}{2k_0^2}\right]^{1/2}. \tag{3}$$

Linear stability calculations show that small amplitude oscillations around the matched solution are always stable.[9] Our purpose here, is to investigate what happens when large-amplitude oscillations are taken into consideration. In the next section we first develop an analytical approach to estimate what will be seen later when we move to the appropriate numerical procedures.

B. Large-amplitude mismatched oscillations

To analyze large-amplitude oscillations, we first note that Eqs. (1) and (2) can be derived from a Hamiltonian formalism

$$H(a,p_a;b,p_b)=H_a(a,p_a)+H_b(b,p_b)-2K\ln(a+b), \tag{4}$$

with

$$H_\chi=\frac{p_\chi^2}{2}+\frac{k_0^2\chi^2}{2}+\frac{\epsilon^2}{2\chi^2}, \tag{5}$$

$\chi=a,b$, and

$$\frac{da}{ds}=\frac{\partial H}{\partial p_a}=p_a,\quad \frac{dp_a}{ds}=-\frac{\partial H}{\partial a},$$

$$\frac{db}{ds}=\frac{\partial H}{\partial p_b}=p_b,\quad \frac{dp_b}{ds}=-\frac{\partial H}{\partial b}.$$

It is clear from the Hamiltonian in Eq. (4) that for negligible space-charge forces, i.e., $K\to 0$, the dynamics of a and b become decoupled and nonlinear energy transfer between these degrees of freedom is absent.

As discussed in Sec. I, we are interested in investigating the transport of axisymmetric beams with $a(s)\approx b(s)$ as they undergo large-amplitude breathing oscillations around r_{b0}. For that sake, it is convenient to introduce new canonical variables defined as

$$X_S=(a+b)/\sqrt{2},\quad P_S=(p_a+p_b)/\sqrt{2}, \tag{6}$$

$$X_A=(a-b)/\sqrt{2},\quad P_A=(p_a-p_b)/\sqrt{2}, \tag{7}$$

obtained from the generating function

$$\mathcal{F}(a,b;P_S,P_A)=\frac{(a+b)P_S+(a-b)P_A}{\sqrt{2}}. \tag{8}$$

Note that X_S and P_S are sensitive to symmetric oscillations where $a(s)$ and $b(s)$ oscillate in phase: *breathing* modes. On the other hand, X_A and P_A are sensitive to antisymmetric oscillations where $a(s)$ and $b(s)$ oscillate with opposite phases: *quadrupole-like* modes. The dynamics is then dictated by the following Hamiltonian:

$$H(X_S,P_S;X_A,P_A)=H_S(X_S,P_S)+H_A(X_A,P_A)+H_C(X_S,X_A), \tag{9}$$

where

$$H_S=\frac{P_S^2}{2}+\frac{k_0^2X_S^2}{2}-K\ln X_S^2, \tag{10}$$

$$H_A=\frac{P_A^2}{2}+\frac{k_0^2X_A^2}{2}, \tag{11}$$

Reuse of AIP Publishing content is subject to the terms at: https://publishing.aip.org/authors/rights-and-permissions. Downloaded to IP: 143.54.44.137 On: Wed, 04 May 2016 17:19:57

$$H_C = 2\epsilon^2 \frac{X_S^2 + X_A^2}{(X_S^2 - X_A^2)^2}. \tag{12}$$

Observe that for high-brightness beams—when emittance effects are negligible ($\epsilon \to 0$)—the coupling Hamiltonian H_C vanishes. In this case, the symmetric and antisymmetric oscillations become uncoupled and integrable, and energy transfer between these degrees of freedom is absent. Thus, we note that in both limiting cases—when emittance effects are negligible or when space-charge effects are negligible—the pertinent degrees of freedom are decoupled and no energy is transferred between them.

In the new variables the matched solution is given by

$$X_S(s) = X_{S0} \equiv \left[\frac{K + (K^2 + 4k_0^2\epsilon^2)^{1/2}}{k_0^2} \right]^{1/2}, \tag{13}$$

$X_A(s) = P_A(s) = P_S(s) = 0$. This corresponds to the minimum *energy H*, obtained by imposing that the Hamiltonian derivatives with respect to all canonical variables vanish. In this sense, mismatched oscillations are excess energy given to the system. In general, this excess energy may appear as oscillations in both symmetric and antisymmetric degrees of freedom, and the nonlinear coupling created by H_C may induce exchange of energy between the two modes. Hence, an initially round beam undergoing breathing oscillations may, in principle, start developing a quadrupole-like instability with an exponential growth of X_A as energy is transferred from symmetric to antisymmetric oscillations. Eventually, the growth nonlinearly saturates and the excess energy starts bouncing back and forth from one mode to the other with the beam cross section alternating from circular to elliptical. To investigate the possible onset of this energy exchange, let us consider a *quasi*-axisymmetric beam with $X_A, P_A \approx 0$ and expand Hamiltonian (9). To leading order in X_A and P_A we obtain that the symmetric and antisymmetric dynamics are dictated, respectively, by

$$\mathcal{H}_S(X_S, P_S) = \frac{P_S^2}{2} + \frac{k_0^2 X_S^2}{2} - 2K \ln X_S + \frac{2\epsilon^2}{X_S^2}, \tag{14}$$

$$\mathcal{H}_A(X_A, P_A, s) = \frac{P_A^2}{2} + \frac{\omega^2(s) X_A^2}{2}, \tag{15}$$

where $\omega^2(s) \equiv k_0^2 + 12\epsilon^2 / X_S^4(s)$. In Eq. (15), $X_S(s)$ is to be regarded as a particular solution obtained from Hamiltonian (14). Note that we have made no restriction on the $X_S(s)$, $P_S(s)$ dynamics.

Let us first examine the symmetric oscillations determined by Eq. (14). $\mathcal{H}_S$ is an autonomous one-degree-of-freedom Hamiltonian that is known to be completely integrable, yielding regular periodic trajectories for $X_S(s)$. These trajectories can be seen in a level plot of $\mathcal{H}_S(X_S, P_S)$ as in Fig. 1. There is one equilibrium solution corresponding to the matched solution with $X_S = X_{S0}$, $P_S = 0$. Surrounding it we find trajectories corresponding to mismatched solutions where X_S oscillates between a maximum $X_{S\,\max}$ and a minimum $X_{S\,\min}$ with a given periodicity. To label different

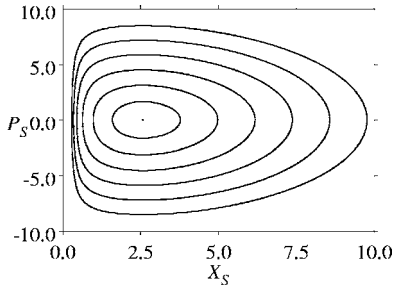

FIG. 1. Integrable orbits of the symmetric motion in the absence of antisymmetric dynamics ($X_A = 0 = P_A$) obtained from Hamiltonian $\mathcal{H}_S$ in Eq. (14).

mismatched solutions, we define a mismatch amplitude as $\nu \equiv X_{S\max}/X_{S0} \geq 1$. Although we cannot write general analytic expressions for $X_S(s)$ some important characteristics of its motion are known.[21] For instance, the wave vector $k_S(\nu)$ measuring the periodicity of each orbit varies from a minimum value $k_{S\,\min} = k_S(\nu = 1) = [K^2 + 4k_0^2\epsilon^2 - K(K^2 + 4k_0^2\epsilon^2)^{1/2}]^{1/2}/\epsilon$ for small linear oscillations around the matched solution to a maximum value $k_{S\,\max} = k_S(\nu \to \infty) = 2k_0$ as large mismatch amplitude orbits are considered.[7] This latter class of orbits is of particular relevance here and can be roughly described as harmonic-oscillator trajectories blocked at $X_S \approx 0$.[22] This is so because while for large X_S the focusing term in (14) (proportional to k_0^2) dominates over space-charge and emittance terms (proportional to K and ϵ^2, respectively) and X_S moves harmonically, for X_S small, K and ϵ terms become dominant, acting as defocusing forces that rapidly reflect X_S back to increasing values.

As for the antisymmetric oscillations, Hamiltonian $\mathcal{H}_A$ in Eq. (15) describes an harmonic-oscillator-type system with a *time-varying frequency* $\omega^2(s)$. Therefore, X_A dynamics is dictated by a Hill's equation that is known to present unstable solutions depending on the specific form of $\omega^2(s)$.[23] For the case of interest here, linear calculations readily show that for vanishing small amplitude oscillations around the matched solution ($\nu \to 1$) the system is always stable because antisymmetric and symmetric degrees of freedom are not resonantly coupled,[9] such that $\omega^2(s)$ can be simply replaced by an effective frequency $\omega_{\text{eff}}^2 \approx k_0^2 + 12\epsilon^2/X_{S0}^4$. However, if we consider large mismatch amplitudes, the scenario may change significantly. $X_S(s)$ then assumes the blocked harmonic-oscillator-like trajectory discussed previously. When X_S is large and moving harmonically, its dynamics does not affect X_A because $12\epsilon^2/X_S^4(s) \ll k_0^2$ and $\omega^2 \approx k_0^2$. As X_S gets close to 0 and is reflected by space-charge and emittance forces, $12\epsilon^2/X_S^4(s)$ becomes very large, and an abrupt interaction between symmetric and antisymmetric oscillations takes place. Therefore, instead of the harmonic oscillation with effective frequency ω_{eff} found for small mismatch amplitudes, for large ν the dynamics of X_A is better described by a *free* harmonic oscillator that is periodically affected by a swift, intense drive from X_S dynamics. Despite our lack of knowledge of the exact form of $X_S(s)$, we can estimate how it affects X_A for large mismatch amplitudes by taking into account a simple model. In particular, we replace the impulses impinged by X_S on the dynamics of X_A by Dirac-delta

Reuse of AIP Publishing content is subject to the terms at: https://publishing.aip.org/authors/rights-and-permissions. Downloaded to IP: 143.54.44.137 On: Wed, 04 May 2016 17:19:57

functions; i.e., we assume in the model that the frequency in Eq. (15) is

$$\omega^2(s) = k_0^2 + h\sum_{n=1}^{\infty} \delta(s - nS), \tag{16}$$

where

$$S \equiv \frac{2\pi}{k_S(\nu)} = 2\int_{X_{S\,\min}}^{X_{S\,\max}} \frac{dX_S}{\mathcal{P}_S(X_S)} \tag{17}$$

is the period of the mismatched orbit and

$$h \equiv 12\epsilon^2 \int_s^{s+S} \frac{ds}{X_S^4} = 24\epsilon^2 \int_{X_{S\,\min}}^{X_{S\,\max}} \frac{dX_S}{X_S^4 \mathcal{P}_S(X_S)} \tag{18}$$

is the effective amplitude of each kick. In Eqs. (17) and (18), the function $\mathcal{P}_S(X_S)$ is given by

$$\mathcal{P}_S(X_S) = \frac{[(\nu^2 X_{S0}^2 - X_S^2)(\nu^2 k_0^2 X_S^2 X_{S0}^2 - 4\epsilon^2) - 4K\nu^2 X_S^2 X_{S0}^2 \ln(\nu X_{S0}/X_S)]^{1/2}}{\nu X_S X_{S0}}, \tag{19}$$

and represents the canonical momentum obtained from the constant Hamiltonian $\mathcal{H}_S$ for an orbit with a mismatch parameter ν, i.e., that contains the phase-space point $X_S = \nu X_{S0}$, $P_S = 0$. $X_{S\,\min}$ and $X_{S\,\max} = \nu X_{S0}$ are zeroes of $\mathcal{P}_S(X_S)$. Note that S and h are functions of the parameters of the system; namely, k_0, K, ϵ, and ν. Aside from the kicks, the antisymmetric motion is a harmonic oscillator with $\omega^2(s) = k_0^2$ and it is convenient to introduce canonical action-angle variables (J, θ) defined by

$$X_A = \sqrt{\frac{2J}{k_0}} \cos\,\theta, \tag{20}$$

$$P_A = -\sqrt{2k_0 J} \sin\,\theta, \tag{21}$$

such that J is constant and $d\theta/ds = k_0$ between two consecutive kicks.[24] At a kick, J and θ suffer a discontinuous variation that can be calculated from the dynamics generated by Hamiltonian (15) and Eqs. (20) and (21). A symplectic mapping based on successive applications of appropriate canonical transformations can thus be constructed that gives the action angle variables (J_{n+1}, θ_{n+1}) right after the $(n+1)$th kick as a function of their values (J_n, θ_n) right after the nth kick. The mapping reads

$$J_{n+1} = J_n \left\{ 1 + \frac{h^2 \cos^2(\theta_n + k_0 S) + h k_0 \sin[2(\theta_n + k_0 S)]}{k_0^2} \right\}, \tag{22}$$

$$\theta_{n+1} = \tan^{-1}\left[\tan(\theta_n + k_0 S) + \frac{h}{k_0} \right]. \tag{23}$$

Equation (22) tells us that depending on the particular value of the phase θ_n, the action variation due to the kick, $J_{n+1} - J_n$, may be positive or negative. In other words, during each swift interaction of X_A and X_S, the antisymmetric oscillation amplitude may increase or decrease depending on the relative phase of their motion. If the phase wanders from 0 to 2π as the beam propagates, we expect no net energy to be transferred into the antisymmetric degree of freedom. If, on the other hand, a coherent interaction occurs with θ_n going towards a fixed value, an unstable growth of antisymmetric oscillations may take place. An inspection of Eqs. (22) and (23) leads to the conclusion that at least one attracting fixed point of θ_n corresponding to an increasing J_n is present when the effective amplitude h exceeds a threshold value

$$h^* = -2k_0 \tan\left(\frac{k_0 S}{2}\right). \tag{24}$$

In the derivation of Eq. (24), it has been used the fact that for any set of parameters $\pi < k_0 S < \sqrt{2}\pi$, what can be inferred from the limiting values of $k_{S\,\max}$ and $k_{S\,\min}$. Later on, the condition $h > h^*$ for which effective energy exchange between symmetric and antisymmetric modes take place will be tested against results obtained by direct integration of the envelope equations, but it is already possible to verify two limiting cases discussed previously. On one hand, when emittance effects are negligible there is no energy exchange because symmetric and antisymmetric oscillations are decoupled; the model agrees with that because $h \to 0$ for $\epsilon \to 0$ from the definition of h. On the other hand, when space-charge effects are negligible the energy exchange is absent because $a(s)$ and $b(s)$ oscillations are decoupled; the model agrees again because as $K \to 0$, all mismatched orbits oscillate around X_{S0} with period $S \to \pi/k_0$ (this can be verified from the values of $k_{S\,\max}$ and $k_{S\,\min}$) and $h^* \to \infty$.

III. NUMERICAL ANALYSIS OF THE ENVELOPE EQUATIONS

In this section we investigate the results obtained by direct integration of the envelope equations. The analysis is simplified if we normalize quantities according to

$$k_0 s \to s, \quad (k_0/\epsilon)^{1/2} X_{S,A} \to X_{S,A}. \tag{25}$$

We are then left with only one parameter in the equations

Reuse of AIP Publishing content is subject to the terms at: https://publishing.aip.org/authors/rights-and-permissions. Downloaded to IP: 143.54.44.137 On: Wed, 04 May 2016 17:19:57

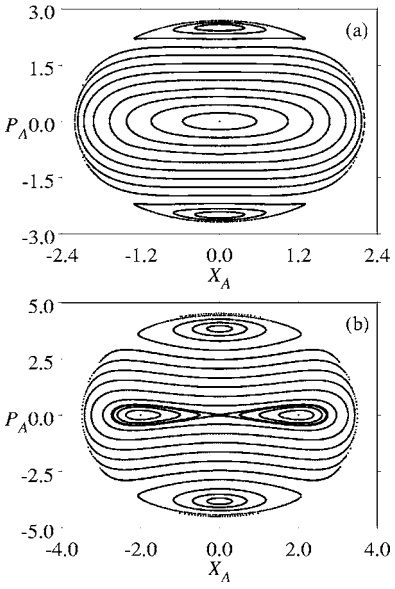

FIG. 2. Poincaré plots of the phase space (X_A, P_A) obtained from Hamiltonian (9). The parameters are $\eta=3.0$, $\nu=1.8$ in (a) and $\eta=3.0$, $\nu=2.4$ in (b). η is defined in Eq. (26).

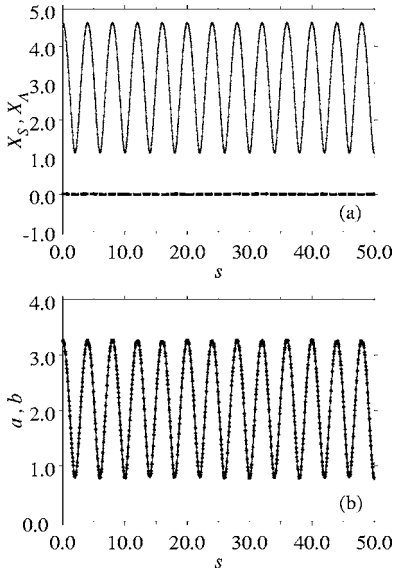

FIG. 3. Evolution of the envelopes obtained by direct integration of the envelope equations for an initially *quasi*-axisymmetric beam with $X_S(0)=\nu X_{S0}$, $P_S(0)=0=P_A(0)$, and a small $X_A(0)=10^{-2}$. In (a), X_S and X_A are represented by the solid and dashed lines, respectively. In (b), a and b are represented by the solid and dashed lines, respectively; note that in this case, a and b curves nearly coincide. The parameters are the same as in Fig. 2(a), which presents a stable fixed point at $X_A=P_A=0$, corresponding to the absence of energy exchange between the modes. a and b are normalized to $(\epsilon/k_0)^{1/2}$, the same way X_S and X_A are [see Eq. (25)].

$$\eta \equiv \frac{K}{k_0 \epsilon}, \tag{26}$$

which measures the relative strength of space-charge to emittance effects—when $\eta \ll 1$ the beam is emittance-dominated, whereas when $\eta \gg 1$, it is space-charge dominated. From what has been discussed, we know that both limits $\eta \to 0$ and $\eta \to \infty$ are integrable and lead to no energy exchange between the relevant degrees of freedom. Note that in the normalized quantities, the matched solution corresponds to

$$X_{S0} = \left[\frac{\eta}{2} + \left(\frac{\eta^2}{4} + 1 \right)^{1/2} \right]^{1/2}. \tag{27}$$

We begin our investigation by analyzing the $(X_S, P_S; X_A, P_A)$ phase space. Because this is a two-degrees-of-freedom system, Poincaré plots[24] come in order. We choose to plot (X_A, P_A) each time X_S is maximum, i.e., $P_S=0$ with $dP_S/ds<0$, which is sufficient to ensure uniqueness of trajectories in our plots. The initial conditions for a single plot have to be picked such that all lead to the same value of Hamiltonian H in Eq. (9). Therefore, we first consider the axisymmetric solution with mismatch amplitude ν and compute its corresponding Hamiltonian value $H(\nu)$. We then seek for other orbits with the same $H(\nu)$. As mentioned before, the matched solution corresponds to the minimum of the Hamiltonian, i.e., $H(\nu>1)>H(\nu=1)$, and it is the excess energy that allows for the coupling between symmetric and antisymmetric oscillations. In Fig. 2, we present phase-space plots obtained for $\eta=3.0$ and different values of the mismatch amplitude ν. In the plots the axisymmetric periodic breathing-beam solution corresponds to the fixed point at the origin $X_A=P_A=0$. In Fig. 2(a), for $\nu=1.8$, the phase-space presents some nonlinear features, such as resonant islands. Notwithstanding, the resonances are far from the fixed point and do not compromise its stability because nearby trajectories just rotate around it with no increase in X_A and P_A amplitudes. However, if we increase the mismatch amplitude to $\nu=2.4$, as in Fig. 2(b), we notice that the axisymmetric solution becomes unstable and any small ellipticity of the beam will grow to large X_A. In other words, the initial symmetric oscillation actively exchanges energy with the antisymmetric mode inducing its growth. If we zoom in the fixed point vicinity (not shown), we see that it is immersed in a chaotic region with many high-order nonlinear resonances surrounding it. By further increasing ν, we found that the axisymmetric solution remains unstable and the chaotic region expands in the phase space.

To illustrate the onset of the nonlinear energy exchange between the modes and how it may affect the beam transport, we compare in Figs. 3 and 4 the evolution of $X_S(s)$, $X_A(s)$, $a(s)$, and $b(s)$ for initially quasi-axisymmetric beams when energy exchange is absent and present, respectively. More specifically, we launch beams with $X_S(0)=\nu X_{S0}$, $P_S(0)=0=P_A(0)$, and a small $X_A(0)=10^{-2}$, and integrate the envelope equations up to $s=50.0$. In Fig. 3, it is shown the results for $\eta=3.0$ and $\nu=1.8$, which are the same parameters as in Fig. 2(a) that corresponds to a stable fixed point in the Poincare plot. Figure 3(a) shows that there is no effective coupling between symmetric and antisymmetric degrees of freedom, such that the energy of the breathing beam is never transferred into nonaxisymmetric oscillations, and X_A is always close to zero. Because of that, a and b are basically the same throughout the simulation and we can hardly distinguish one curve from the other in Fig. 3(b). Figure 4 shows the results for $\eta=3.0$ and $\nu=2.4$, which are the same parameters as in Fig. 2(b), corresponding to a case wherein the breathing os-

Reuse of AIP Publishing content is subject to the terms at: https://publishing.aip.org/authors/rights-and-permissions. Downloaded to IP: 143.54.44.137 On: Wed, 04 May 2016 17:19:57

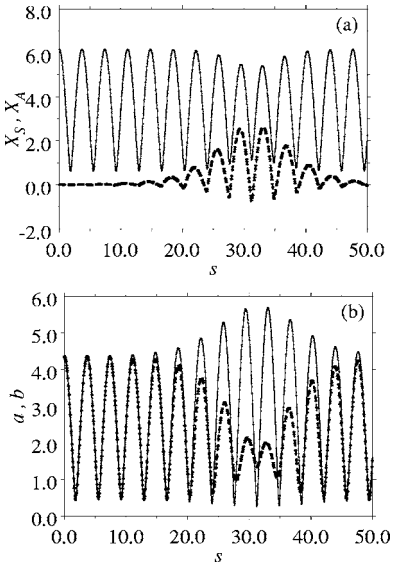

FIG. 4. Equivalent to Fig. 3, but here the parameters are the same as in Fig. 2(b) which presents an unstable fixed point at $X_A=P_A=0$, corresponding to the occurrence of an effective energy exchange between the modes.

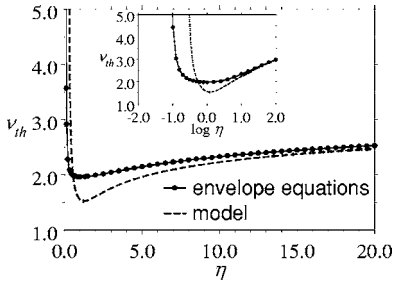

FIG. 5. The threshold mismatch amplitude ν_{th} above which the quadrupole-like mode becomes unstable as a function of the parameter η defined in Eq. (26). The linked circles are the results obtained by direct integration of the envelope equations (1) and (2), and the dashed line is the result obtained from the model [see Eqs. (16)–(18) and (24)]. The inset presents the results as a function of ln η in order to show the small-η regime in more detail.

cillations of an initially round beam—represented by the fixed point in Fig. 2(b)—become unstable. Now, it is clear from Fig. 4(a) that there is an effective coupling between symmetric and antisymmetric degrees of freedom. As the beam starts oscillating, the initially small X_A starts growing at the expenses of the symmetric energy that is damped in order to preserve the total *energy* in Hamiltonian (9). Around $s=30$, X_A growth nonlinearly saturates and the energy begins to return to the symmetric oscillations. For longer s, the energy keeps going back and forth from symmetric to antisymmetric degrees of freedom as a consequence of their effective coupling. Fig. 4(b) shows that X_A growth corresponds to an increasing disparity in the beam sizes along the two transverse directions, with the beam cross section becoming an ellipse with increasing eccentricity. In fact, the ratio a/b grows from very close to the unity for $s=0.0$ to about 3 around $s=30.0$. Note also that as the beam becomes *more* elliptic, the size along one transverse direction tends to grow. In Fig. 4(b), this growth is on the order of 30% and could be responsible, for instance, for an enhance in particle loss if walls surrounding the beam were taken into account.

In qualitative agreement with the model discussed in Sec. II B, the phase-space analysis shows that antisymmetric oscillations indeed become unstable with an initial exponential growth of X_A for some large-amplitude mismatched beam. In particular, there is a threshold mismatch amplitude ν_{th} above which instability takes place. To determine with more accuracy ν_{th} and how it varies with η, we adopt the following procedure. For a given η, we integrate numerically over a long propagation length s_f the coupled envelope equations for initial conditions of the form $X_S(0)=\nu X_{S0}$, $P_S(0)=0$, and $J(0)=[X_A^2(0)+P_A^2(0)]/2=J_0 \ll 1$. If during the integration $J(s)=[X_A^2(s)+P_A^2(s)]/2$ exceeds J_0 by a large factor λ, i.e., $J(s)>\lambda J_0$, we consider the solution to be unstable; if not, the solution is considered stable. By ratcheting up ν from 1, we determine $\nu_{\text{th}}(\eta)$ as the minimum value for which the solution is unstable. Specifically, we take $s_f=100$, $J_0=10^{-3}$, and $\lambda=100$. The results are presented in Fig. 5 by the circles connected by a solid curve. ν_{th} increases in both limits $\eta \to 0$ and $\eta \to \infty$, as expected, presenting a minimum $\nu_{\text{th}} \approx 1.96$ close to $\eta=1$. For $\eta<1$, it steeply increases; hence, the nonlinear mode coupling is expected to have little effect on tenuous beams where space-charge effects are small. This is confirmed if one analyzes the envelope evolution in this regime, which shows that even when the nonlinear energy exchange occurs, X_A growth is typically very small. On the other hand, ν_{th} increases much more slowly for $\eta>1$. In fact, it grows less than 30% of its minimum value as we move to very intense beams with $\eta=20.0$. Therefore, devices that operate with space-charge-dominated beams undergoing large-amplitude mismatched oscillations are likely to be affected by the nonlinear mode coupling.

In order to verify the validity of the mechanism described in Sec. II B for the onset of the energy exchange between symmetric and antisymmetric modes, we determine $\nu_{\text{th}}(\eta)$ from the model developed there. We solve the X_S integrals in Eqs. (17) and (18) to find S and h, and determine ν_{th} from the condition $h=h^*$. The results are presented by the dashed curve in Fig. 5. As seen in the figure, the model is very accurate for large η which corresponds to space-charge-dominated beams. For small η the agreement is poor, as observed in the inset of the figure, which shows the results as a function of ln η. Nevertheless, the model still predicts the steep increase of ν_{th} in this regime, indicating that the nonlinear mode coupling is expected to have little effect on tenuous beams as discussed previously.

IV. CONCLUSIONS

We performed a nonlinear analysis of the transport of beams in continuous magnetic focusing fields taking into consideration nonaxisymmetric effects. In particular, we investigated the nonlinear coupling between breathing and quadrupole-like modes based on envelope equations. It was shown that large-amplitude breathing oscillations caused by some sort of mismatch may nonlinearly couple to quadrupole-like oscillations for an initially *quasi*-axisymmetric beam. In this case, the excess energy initially constrained to the axisymmetric breathing oscillations is al-

Reuse of AIP Publishing content is subject to the terms at: https://publishing.aip.org/authors/rights-and-permissions. Downloaded to IP: 143.54.44.137 On: Wed, 04 May 2016 17:19:57

lowed to flow back and forth between breathing and quadrupole-like oscillations, with the beam developing an elliptical shape with a possible increase in its size along one direction as the beam is transported. Generally, this may induce beam losses, which are enhanced if conducting wall effects are taken into account,[17] and may also induce a detuning in the wave-beam interaction in high-power microwave tubes. This nonlinear process was found to be particularly relevant for space-charge-dominated beams with $K \gtrsim k_0 \epsilon$ and occurs for large mismatch amplitudes on the order of 100% ($\nu \simeq 2$), which are compatible, for instance, to mismatches induced by current oscillations in high-power microwave sources.[18] A simple model was developed to clarify the basic mechanism that leads to the energy exchange between the modes and was tested numerically against results obtained from direct integration of the envelope equations. It is worth mentioning that for beams with large mismatch amplitudes, effects such as instabilities[5,13,14] and halo formation[15] are generally expected to occur. Hence, in practice these effects will compete with the nonlinear mode coupling investigated here. To determine for which system parameters and applications which of these phenomena prevails is an interesting point that deserves further analysis.

ACKNOWLEDGMENTS

We acknowledge financial support from the Brazilian agencies CNPq and FAPERGS, and from the U.S. Air Force Office of Scientific Research Grant No. FA9550–06–1–0345.

[1] *High-Power Microwave Generation*, edited by E. Schamiloglu and Y. Y. Lau, Special issue, IEEE Trans. Plasma Sci., **26**, 232 (1998).
[2] *Space Charge Dominated Beams and Applications of High-Brightness Beams*, edited by S. Y. Lee, AIP Conf. Proc. **377**, 3 (1996).
[3] R. A. Jameson, AIP Conf. Proc. **279**, 969 (1993).
[4] F. J. Agee, IEEE Trans. Power Deliv. **26**, 235 (1998).
[5] I. Hofmann, L. J. Laslett, L. Smith, and I. Haber, Part. Accel. **13**, 145 (1983).
[6] C. J. Struckmeier and M. Reiser, Part. Accel. **14**, 227 (1984).
[7] R. Pakter and F. B. Rizzato, Phys. Rev. Lett. **87**, 044801 (2001).
[8] R. C. Davidson and H. Qin, *Physics of Intense Charged Particle Beams in High Energy Accelerators* (World Scientific, Singapore, 2001).
[9] S. M. Lund and B. Bukh, Phys. Rev. ST Accel. Beams **7**, 024801 (2004).
[10] J. S. Moraes, R. Pakter, F. B. Rizzato, and C. Chen, Phys. Scr., T **107**, 145 (2004).
[11] J. S. Moraes, R. Pakter, and F. B. Rizzato, Phys. Rev. Lett. **93**, 244801 (2004).
[12] C. Chen and R. C. Davidson, Phys. Rev. Lett. **72**, 2195 (1994).
[13] R. L. Gluckstern, W.-H. Cheng, and H. Ye, Phys. Rev. Lett. **75**, 2835 (1995).
[14] R. L. Gluckstern, W.-H. Cheng, S. S. Kurennoy, and H. Ye, Phys. Rev. E **54**, 6788 (1996).
[15] R. L. Gluckstern, Phys. Rev. Lett. **73**, 1247 (1994).
[16] A. Riabko, M. Ellison, X. Kang, S. Y. Lee, D. Li, J. Y. Liu, X. Pei, and L. Wang, Phys. Rev. E **51**, 3529 (1995).
[17] J. Zhou, B. L. Qian, and C. Chen, Phys. Plasmas **10**, 4203 (2003).
[18] R. Pakter and C. Chen, IEEE Trans. Plasma Sci. **28**, 502 (2000).
[19] I. M. Kapchinskij and V. V. Vladimirskij, in *Proceedings of the International Conference on High Energy Accelerators* (CERN, Geneva, 1959), p. 274.
[20] P. M. Lapostolle, IEEE Trans. Nucl. Sci. **NS-18**, 1101 (1971); F. J. Sacherer, IEEE Trans. Nucl. Sci. **NS-18**, 1105 (1971).
[21] R. Pakter and F. B. Rizzato, Phys. Rev. E **65**, 056503 (2002).
[22] F. B. Rizzato and R. Pakter, Phys. Rev. Lett. **89**, 184102 (2002).
[23] H. Wiedemann, *Particle Accelerator Physics I—Basic Principles and Linear Beam Dynamics* (Springer, Heidelberg, 2003).
[24] A. J. Lichtenberg and M. A. Lieberman, *Regular and Stochastic Motion* (Springer, New York, 1992).

Reuse of AIP Publishing content is subject to the terms at: https://publishing.aip.org/authors/rights-and-permissions. Downloaded to IP: 143.54.44.137 On: Wed, 04 May 2016 17:19:57